

Higher-Order DGFEM Transport Calculations on Polytope Meshes for Massively-Parallel Architectures

Michael W. Hackemack

Chair: Jean C. Ragusa

Committee Members: Marvin L. Adams, Jim E. Morel, Nancy M. Amato

External Advisor: Troy Becker

Department of Nuclear Engineering
Texas A&M University
College Station, TX, USA 77843
mike.hack@tamu.edu



Outline

1 Overview

- The DGFEM S_N Transport Equation
- Polytope Grid Motivation

2 Polytope Finite Element Basis Functions

- Linear Basis Functions on 2D Polygons
- Quadratic Serendipity Basis Functions on 2D Polygons
- Linear Basis Functions on 3D Polyhedra

3 Diffusion Synthetic Acceleration on Polytopes

- Theory
- MIP Diffusion Form

4 Proposed Work and Current Status

5 Ongoing Work

The Continuous-Energy Transport Equation

Transport Equation

$$[\Omega \cdot \nabla + \sigma_t(\mathbf{r}, E)] \psi(\mathbf{r}, E, \Omega) = \int_{4\pi} \int_0^\infty \sigma_s(\mathbf{r}, E', E, \Omega', \Omega) \psi(\mathbf{r}, E', \Omega') dE' d\Omega' + Q(\mathbf{r}, E, \Omega)$$

Boundary Conditions

$$\psi(\mathbf{r}, E, \Omega) = \psi^{inc}(\mathbf{r}, E, \Omega) + \int_{4\pi} \int_0^\infty \beta(\mathbf{r}, E', E, \Omega', \Omega) \psi(\mathbf{r}, E', \Omega') dE' d\Omega'$$

Term Definitions

\mathbf{r} - neutron position

E - neutron energy

Ω - neutron solid angle

$\psi(\mathbf{r}, E, \Omega)$ - angular flux

$Q(\mathbf{r}, E, \Omega)$ - distributed neutron source

$\sigma_t(\mathbf{r}, E)$ - total macroscopic cross section

$\sigma_s(\mathbf{r}, E', E, \Omega', \Omega)$ - total macroscopic scattering cross section

$\beta(\mathbf{r}, E', E, \Omega', \Omega)$ - boundary albedo

Energy and Angular Discretization

Spatial Discretization

Iterative Procedure

Classic Source Iteration

$$\Psi^{(\ell+1)} = \mathbf{L}^{-1} \left(\mathbf{M} \Sigma \Phi^{(\ell)} + \mathbf{Q} \right)$$

$$\Phi^{(\ell+1)} = \mathbf{D} \mathbf{L}^{-1} \left(\mathbf{M} \Sigma \Phi^{(\ell)} + \mathbf{Q} \right)$$

$$\Phi = \mathbf{D} \Psi$$

Operator Terms

\mathbf{L} - streaming + collision operator

\mathbf{M} - moment-to-discrete operator

\mathbf{D} - discrete-to-moment operator

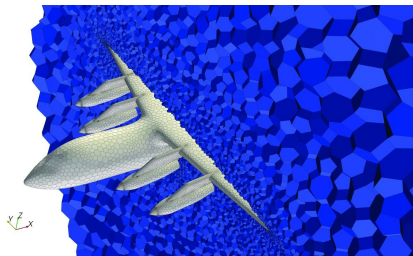
Σ - scattering operator

Transport Sweep

The operation \mathbf{L}^{-1} can be performed in myriad ways. For this work, we will use the matrix-free, full-domain transport sweep.

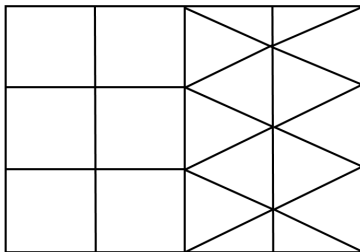
Polytope Grid Motivation

- Other physics communities are now employing polytope grids due to decreased cell/face counts (CFD in particular)
- They allow for transition elements between different domain regions
- Hanging nodes from non-conforming meshes are not necessary
- Independently-generated simplicial grids (*i.e.* created in parallel) can be stitched together with polytopes without communicating the whole mesh across processors



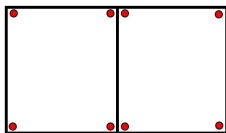
Polytope Grid Motivation

- Other physics communities are now employing polytope grids due to decreased cell/face counts (CFD in particular)
- They allow for transition elements between different domain regions
- Hanging nodes from non-conforming meshes are not necessary
- Independently-generated simplicial grids (*i.e.* created in parallel) can be stitched together with polytopes without communicating the whole mesh across processors

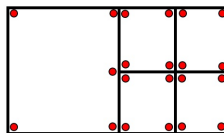


Polytope Grid Motivation

- Other physics communities are now employing polytope grids due to decreased cell/face counts (CFD in particular)
- They allow for transition elements between different domain regions
- Hanging nodes from non-conforming meshes are not necessary
- Independently-generated simplicial grids (*i.e.* created in parallel) can be stitched together with polytopes without communicating the whole mesh across processors



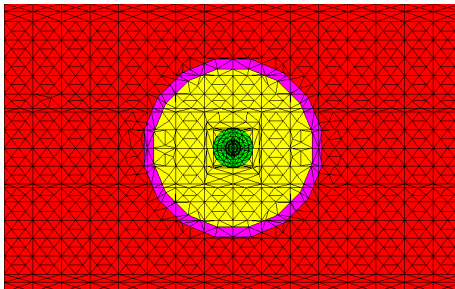
(a)



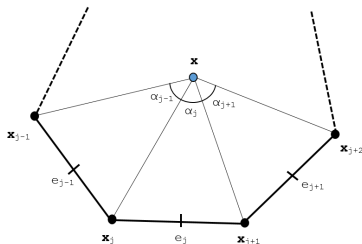
(b)

Polytope Grid Motivation

- Other physics communities are now employing polytope grids due to decreased cell/face counts (CFD in particular)
- They allow for transition elements between different domain regions
- Hanging nodes from non-conforming meshes are not necessary
- Independently-generated simplicial grids (*i.e.* created in parallel) can be stitched together with polytopes without communicating the whole mesh across processors



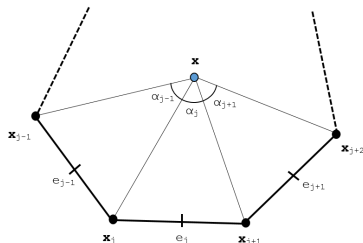
Linear Basis Functions on 2D Polygons



Basis Function Properties - Barycentric Coordinates

- 1 $\lambda_i \geq 0$
- 2 $\sum_i \lambda_i = 1$
- 3 $\sum_i \mathbf{x}_i \lambda_i(\mathbf{x}) = \mathbf{x}$
- 4 $\lambda_i(\mathbf{x}_j) = \delta_{ij}$

Wachspress Rational Functions

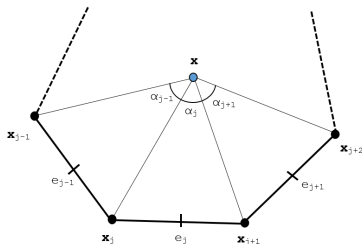


$$\lambda_i^w(\mathbf{x}) = \frac{w_i(\mathbf{x})}{\sum_j w_j(\mathbf{x})}, \quad w_j(\mathbf{x}) = \frac{A(\mathbf{x}_{j-1}, \mathbf{x}_j, \mathbf{x}_{j+1})}{A(\mathbf{x}, \mathbf{x}_{j-1}, \mathbf{x}_j) A(\mathbf{x}, \mathbf{x}_j, \mathbf{x}_{j+1})}$$

$$A(\mathbf{x}_1, \mathbf{x}_2, \mathbf{x}_3) = \frac{1}{2} \begin{vmatrix} 1 & 1 & 1 \\ x_1 & x_2 & x_3 \\ y_1 & y_2 & y_3 \end{vmatrix}$$

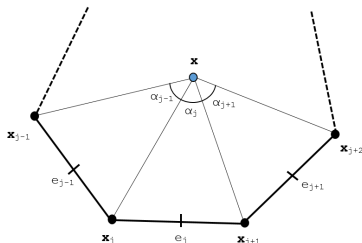
Piecewise Linear (PWL) Functions

Mean Value Coordinates



$$\lambda_i^{MV}(\mathbf{x}) = \frac{w_i(\mathbf{x})}{\sum_j w_j(\mathbf{x})}, \quad w_j(\mathbf{x}) = \frac{\tan(\alpha_{j-1}/2) + \tan(\alpha_j/2)}{|\mathbf{x}_j - \mathbf{x}|}$$

Maximum Entropy Coordinates



$$\lambda_i^{ME}(\mathbf{x}) = \frac{w_i(\mathbf{x})}{\sum_j w_j(\mathbf{x})}, \quad w_j(\mathbf{x}) = m_j(\mathbf{x}) \exp(-\omega^* \cdot (\mathbf{x}_j - \mathbf{x}))$$

$$\omega^* = \operatorname{argmin} F(\omega, \mathbf{x}) \quad F(\omega, \mathbf{x}) = \ln \left(\sum_j w_j(\mathbf{x}) \right)$$

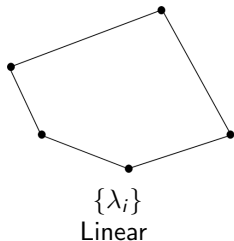
Summary of the 2D Linear Basis Functions

Basis Function	Dimension	Polytope Types	Analytical/Numerical	Direct/Iterative
Wachspress	2D/3D	Convex*	Numerical	Direct
PWL	1D/2D/3D	Convex/Concave	Analytical	Direct
Mean Value	2D**	Convex/Concave	Numerical	Direct
Max Entropy	1D/2D/3D	Convex/Concave	Numerical	Iterative***

- * - weak convexity for Wachspress coordinates does not cause blow up
- ** - mean value 3D analogue only applicable to tetrahedron
- *** - maximum entropy minimization solved via Newton's Method

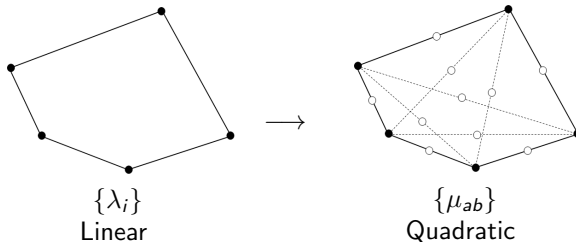
Quadratic Serendipity Basis Functions on 2D Polygons

- 1 Form the linear barycentric functions - $\{\lambda_i\}$
- 2 Construct the pairwise products - $\{\mu_{ab}\}$
- 3 Eliminate the interior nodes to form a serendipity basis - $\{\xi_{ij}\}$



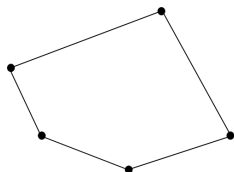
Quadratic Serendipity Basis Functions on 2D Polygons

- 1 Form the linear barycentric functions - $\{\lambda_i\}$
- 2 Construct the pairwise products - $\{\mu_{ab}\}$
- 3 Eliminate the interior nodes to form a serendipity basis - $\{\xi_{ij}\}$

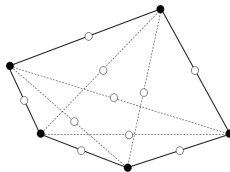


Quadratic Serendipity Basis Functions on 2D Polygons

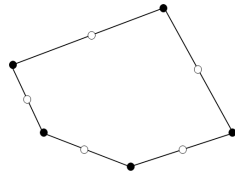
- 1 Form the linear barycentric functions - $\{\lambda_i\}$
- 2 Construct the pairwise products - $\{\mu_{ab}\}$
- 3 Eliminate the interior nodes to form a serendipity basis - $\{\xi_{ij}\}$



$\{\lambda_i\}$
Linear



$\{\mu_{ab}\}$
Quadratic



$\{\xi_{ij}\}$
Serendipity

Pairwise products of the barycentric basis functions

Necessary Precision Properties

$$\sum_{aa \in V} \mu_{aa} + \sum_{ab \in E \cup D} 2\mu_{ab} = 1$$

$$\sum_{aa \in V} \mathbf{x}_{aa} \mu_{aa} + \sum_{ab \in E \cup D} 2\mathbf{x}_{ab} \mu_{ab} = \mathbf{x}$$

$$\sum_{aa \in V} \mathbf{x}_a \mathbf{x}_a^T \mu_{aa} + \sum_{ab \in E \cup D} (\mathbf{x}_a \mathbf{x}_b^T + \mathbf{x}_b \mathbf{x}_a^T) \mu_{ab} = \mathbf{x} \mathbf{x}^T$$

Further Notation

$$\mathbf{x}_{ab} = \frac{\mathbf{x}_a + \mathbf{x}_b}{2}, \quad \mu_{ab} = \lambda_a \lambda_b$$

Eliminate interior nodes to form serendipity basis

Linear Basis Functions on 3D Polyhedra

The diffusion equation is used as our low-order operator

The Diffusion Equation

$$-\nabla \cdot D \nabla \Phi(\mathbf{r}) + \sigma \Phi(\mathbf{r}) = q(\mathbf{r}), \quad \mathbf{r} \in \mathcal{D}$$

General Boundary Conditions

$$\begin{aligned} \Phi(\mathbf{r}) &= \Phi_0(\mathbf{r}), & \mathbf{r} \in \partial \mathcal{D}^d \\ -D \partial_n \Phi(\mathbf{r}) &= J_0(\mathbf{r}), & \mathbf{r} \in \partial \mathcal{D}^n \\ \frac{1}{4} \Phi(\mathbf{r}) + \frac{1}{2} D \partial_n \Phi(\mathbf{r}) &= J^{inc}(\mathbf{r}), & \mathbf{r} \in \partial \mathcal{D}^r \end{aligned}$$

Desirable diffusion form properties

- Can handle concave and degenerate polytope cells
- Symmetric Positive-Definite (SPD)
- Availability of suitable preconditioners
- Agnostic of directionality of interior faces

Symmetric Interior Penalty (SIP) Form

Bilinear Form

$$\begin{aligned}
 a(\Phi, b) = & \left\langle D\nabla\Phi, \nabla b \right\rangle_{\mathcal{D}} + \left\langle \sigma\Phi, b \right\rangle_{\mathcal{D}} \\
 & + \left\{ \kappa_e^{SIP} [[\Phi], [b]] \right\}_{E_h^i} - \left\{ [[\Phi], \{ \{ D\partial_n b \} \}] \right\}_{E_h^i} - \left\{ \{ \{ D\partial_n \Phi \} \}, [[b]] \right\}_{E_h^i} \\
 & + \left\{ \kappa_e^{SIP} \Phi, b \right\}_{\partial\mathcal{D}^d} - \left\{ \Phi, D\partial_n b \right\}_{\partial\mathcal{D}^d} - \left\{ D\partial_n \Phi, b \right\}_{\partial\mathcal{D}^d} + \frac{1}{2} \left\{ \Phi, b \right\}_{\partial\mathcal{D}^r}
 \end{aligned}$$

Linear Form

$$\begin{aligned}
 \ell(b) = & \left\langle q, b \right\rangle_{\mathcal{D}} - \left\{ J_0, b \right\}_{\partial\mathcal{D}^n} + 2 \left\{ J_{inc}, b \right\}_{\partial\mathcal{D}^r} \\
 & + \left\{ \kappa_e^{SIP} \Phi_0, b \right\}_{\partial\mathcal{D}^d} - \left\{ \Phi_0, D\partial_n b \right\}_{\partial\mathcal{D}^d}
 \end{aligned}$$

SIP Penalty Coefficient

$$\kappa_e^{SIP} \equiv \begin{cases} \frac{C_B}{2} \left(\frac{D^+}{h^+} + \frac{D^-}{h^-} \right) & , e \in E_h^i \\ C_B \frac{D^-}{h^-} & , e \in \partial\mathcal{D} \end{cases}$$

$$C_B = cp(p+1)$$

c - user defined constant ($c \geq 1$)

p - polynomial order of the finite element basis (1, 2, 3, ...)

$D^{(+/-)}$ - diffusion coefficient defined on the positive/negative side of a face

$h^{(+/-)}$ - orthogonal projection defined on the positive/negative side of a face

$$u^\pm = \lim_{s \rightarrow 0^\pm} u(\mathbf{r} + s\mathbf{n})$$

Modified Interior Penalty (MIP) Form

Diffusion Form

$$\begin{aligned}
& \langle D \nabla \Phi, \nabla b \rangle_{\mathcal{D}} + \langle \sigma \Phi, b \rangle_{\mathcal{D}} \\
& + \left\{ \kappa_e^{MIP} \llbracket \Phi \rrbracket, \llbracket b \rrbracket \right\}_{E_h^i} - \left\{ \llbracket \Phi \rrbracket, \{ \{ D \partial_n b \} \} \right\}_{E_h^i} - \left\{ \{ \{ D \partial_n \Phi \} \}, \llbracket b \rrbracket \right\}_{E_h^i} \\
& + \left\{ \kappa_e^{MIP} \Phi, b \right\}_{\partial \mathcal{D}^{vac}} - \frac{1}{2} \left\{ \Phi, D \partial_n b \right\}_{\partial \mathcal{D}^{vac}} - \frac{1}{2} \left\{ D \partial_n \Phi, b \right\}_{\partial \mathcal{D}^{vac}} \\
& = \langle q, b \rangle_{\mathcal{D}}
\end{aligned}$$

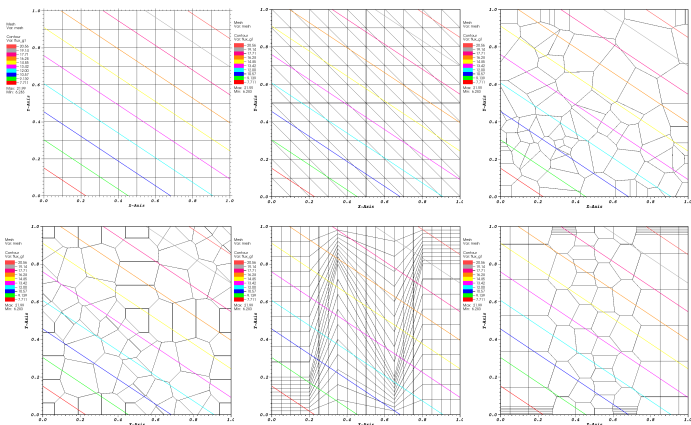
MIP Penalty Term

$$\kappa_e^{MIP} = \max\left(\frac{1}{4}, \kappa_e^{SIP}\right)$$

2D Exactly-Linear Transport Solutions - mean value coordinates

$$\mu \frac{\partial \psi}{\partial x} + \eta \frac{\partial \psi}{\partial y} + \sigma_t \psi = Q(x, y, \mu, \eta)$$

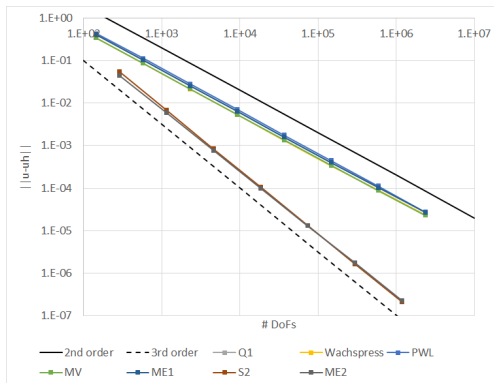
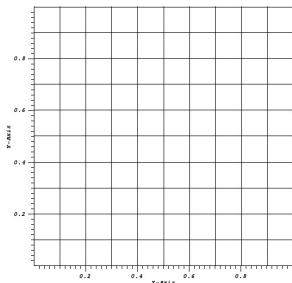
$$\psi(x, y, \mu, \eta) = ax + by + c\mu + d\eta + e, \quad \phi(x, y) = 2\pi(ax + by + e)$$



Convergence rates using MMS for the 2D polygonal basis functions

$$\psi(x, y) = \sin\left(\nu \frac{\pi x}{L_x}\right) \sin\left(\nu \frac{\pi y}{L_y}\right)$$

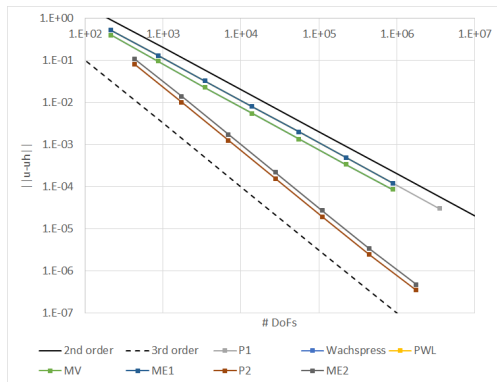
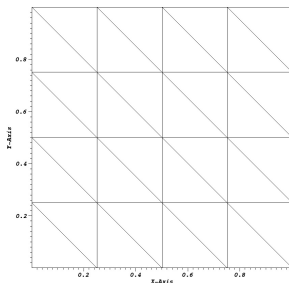
$$\phi(x, y) = 2\pi \sin\left(\nu \frac{\pi x}{L_x}\right) \sin\left(\nu \frac{\pi y}{L_y}\right)$$



Convergence rates using MMS for the 2D polygonal basis functions

$$\psi(x, y) = \sin\left(\nu \frac{\pi x}{L_x}\right) \sin\left(\nu \frac{\pi y}{L_y}\right)$$

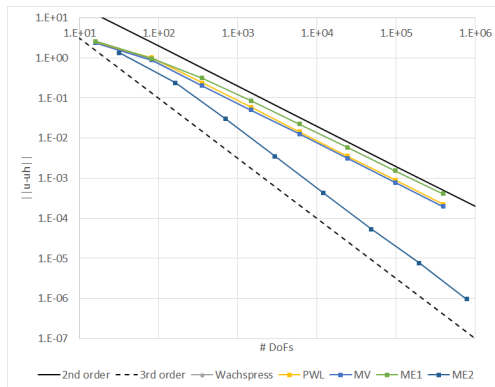
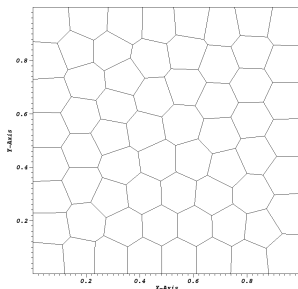
$$\phi(x, y) = 2\pi \sin\left(\nu \frac{\pi x}{L_x}\right) \sin\left(\nu \frac{\pi y}{L_y}\right)$$



Convergence rates using MMS for the 2D polygonal basis functions

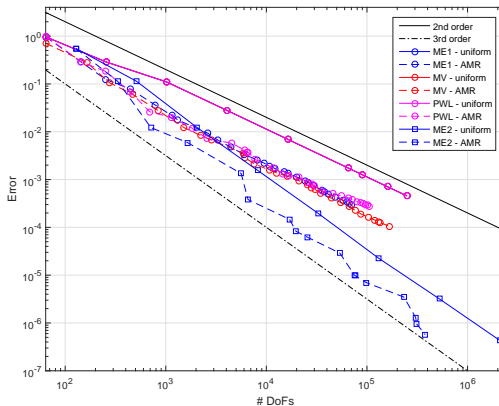
$$\psi(x, y) = \sin\left(\nu \frac{\pi x}{L_x}\right) \sin\left(\nu \frac{\pi y}{L_y}\right)$$

$$\phi(x, y) = 2\pi \sin\left(\nu \frac{\pi x}{L_x}\right) \sin\left(\nu \frac{\pi y}{L_y}\right)$$

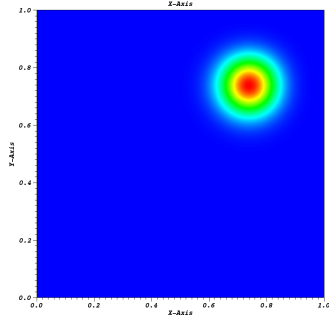
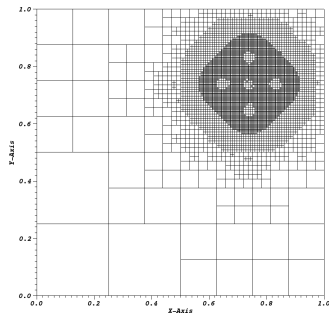
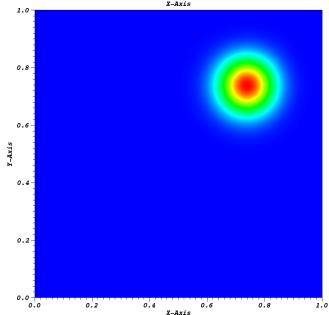
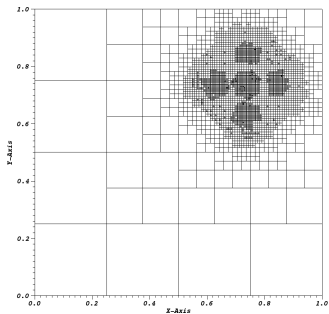


Convergence rates using MMS and AMR for the 2D polygonal basis functions

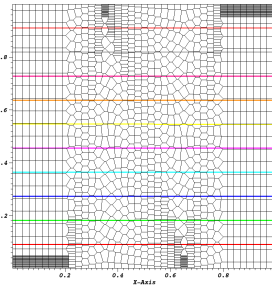
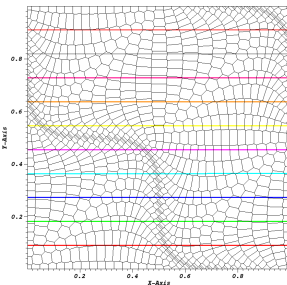
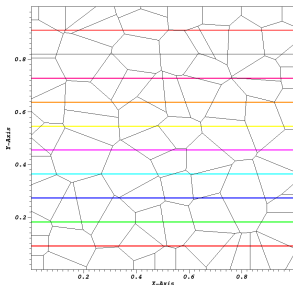
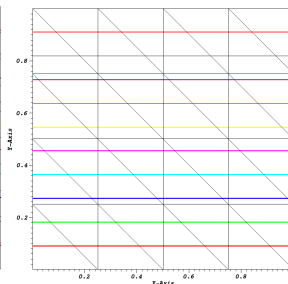
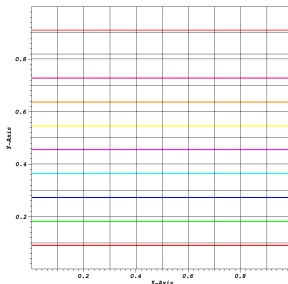
$$\psi(x, y) = x(L_x - x)y(L_y - y) \exp\left(-\frac{(x - x_0)^2 + (y - y_0)^2}{\gamma}\right),$$
$$\phi(x, y) = 2\pi x(L_x - x)y(L_y - y) \exp\left(-\frac{(x - x_0)^2 + (y - y_0)^2}{\gamma}\right)$$



Linear ME cycle 15 (left) and quadratic ME cycle 08 (right)

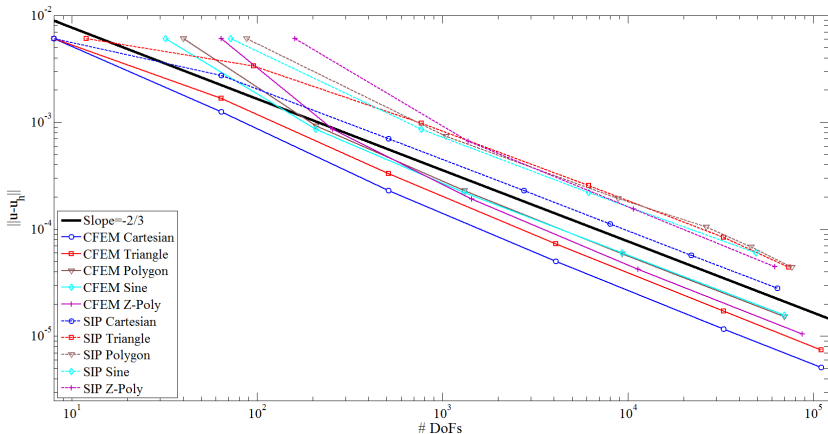


SIP exactly linear solutions on 3D polyhedral meshes using the PWL basis functions



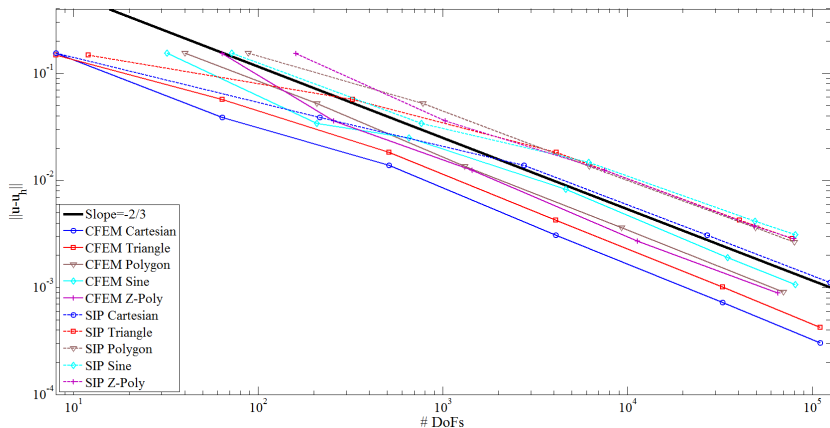
SIP convergence study - quadratic solution on 3D cube using the PWL basis functions

$$\Phi(x, y, z) = xyz(L_x - x)(L_y - y)(L_z - z)$$
$$L_x = L_y = L_z = 1.0$$

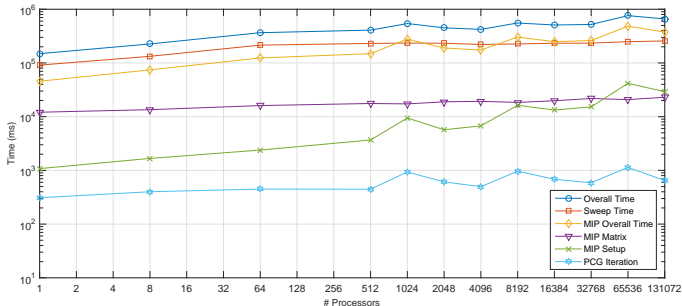


SIP convergence study - gaussian solution on 3D cube using the PWL basis functions

$$\Phi(x, y, z) = xyz(L_x - x)(L_y - y)(L_z - z) \exp(-(\mathbf{r} - \mathbf{r}_0) \cdot (\mathbf{r} - \mathbf{r}_0))$$
$$L_x = L_y = L_z = 1.0, \quad \mathbf{r}_0 = (3/4, 3/4, 3/4)$$



MIP DSA Timing Data with PDT on Vulcan using HYPRE



Problem Description

- Modified Zerr problem - used optimal sweep aggregation parameters
 - homogeneous cube - $c=0.9999$
 - S8 level-symmetric quadrature
- pointwise convergence tolerance of $1e-8$
- precondition with MIP DSA using HYPRE PCG and AMG

Questions?

A special acknowledgment to the Department of Energy Rickover Fellowship Program in Nuclear Engineering, which provides strong support to its fellows and their professional development.



TEXAS A&M 
ENGINEERING

A stretch goal is to compare my method to Monte Carlo

I claim the following is the best way to show our method has practical importance, because continuous-energy Monte Carlo codes do exact particle tracking / kinematics and use very accurate cross sections. Such codes may attain higher fidelity in all respects than DRAGON.

Start with a 0-D problem to isolate energy discretization effects

- 1 Come up with a reactor-themed problem
- 2 Solve the same problem in PDT and MCNP or OpenMC
- 3 Choose QOI, such as k -eigenvalue, radial power profile, absorption/fission rates per nuclide, etc.
- 4 Quantify how errors in PDT's QOI change as energy resolution is increased

Build up problem complexity slowly: cylindricized pin cell with white boundary conditions, infinite lattice of pin cells, heterogeneous lattice of pin cells, etc.

- 1 Quantify how errors in PDT's QOI change as spatial / angular / scattering moment resolution is increased
- 2 Quantify how errors in PDT's QOI change as energy resolution is increased
- 3 ...
- 4 Profit

A stretch goal is to compare my method to Monte Carlo

I claim the following is the best way to show our method has practical importance, because continuous-energy Monte Carlo codes do exact particle tracking / kinematics and use very accurate cross sections. Such codes may attain higher fidelity in all respects than DRAGON.

Start with a 0-D problem to isolate energy discretization effects

- 1 Come up with a reactor-themed problem
- 2 Solve the same problem in PDT and MCNP or OpenMC
- 3 Choose QOI, such as k -eigenvalue, radial power profile, absorption/fission rates per nuclide, etc.
- 4 Quantify how errors in PDT's QOI change as energy resolution is increased

Build up problem complexity slowly: cylindricized pin cell with white boundary conditions, infinite lattice of pin cells, heterogeneous lattice of pin cells, etc.

- 1 Quantify how errors in PDT's QOI change as spatial / angular / scattering moment resolution is increased
- 2 Quantify how errors in PDT's QOI change as energy resolution is increased
- 3 ...
- 4 Profit